A 1H NMR Study of Host/Guest Supramolecular Complexes of a Curcumin Analog with βCyclodextrin and a βCD-conjugated Gemini Surfactant.

ARTICLE *in* MOLECULAR PHARMACEUTICS · JUNE 2015

Impact Factor: 4.38 · DOI: 10.1021/acs.molpharmaceut.5b00261 · Source: PubMed

6 AUTHORS, INCLUDING:

Abdalla Hamisi Karoyo

University of Saskatchewan

8 PUBLICATIONS **48** CITATIONS

SEE PROFILE

Pawel Grochulski

Canadian Light Source Inc. (CLS)

94 PUBLICATIONS **2,879** CITATIONS

SEE PROFILE

Ildiko Badea

University of Saskatchewan

43 PUBLICATIONS **780** CITATIONS

SEE PROFILE

molecular pharmaceutics

Article

pubs.acs.org/molecularpharmaceutics

A ^{1}H NMR Study of Host/Guest Supramolecular Complexes of a Curcumin Analogue with β-Cyclodextrin and a β-Cyclodextrin-Conjugated Gemini Surfactant

Masoomeh Poorghorban,[†] Abdalla H. Karoyo,[‡] Pawel Grochulski,[†,§] Ronald E. Verrall,[‡] Lee D. Wilson,*[,‡] and Ildiko Badea*[,†]

[†]Drug Discovery and Development Research Group, College of Pharmacy and Nutrition, University of Saskatchewan, Saskatoon, Saskatchewan, S7N 5E5, Canada

[‡]Department of Chemistry, University of Saskatchewan, Saskatoon, Saskatchewan, S7N 5C9, Canada

[§]Canadian Light Source, Saskatoon, Saskatchewan, S7N 2 V3, Canada

Supporting Information

ABSTRACT: Host systems based on β-cyclodextrin (βCD) were employed as pharmaceutical carriers to encapsulate a poorly soluble drug, curcumin analogue (NC 2067), in order to increase its water solubility. βCD was chemically conjugated with an amphiphilic gemini surfactant with the ability to self-assemble and to form nanoscale supramolecular structures. The conjugated molecule, βCDgemini surfactant (βCDg), was shown to be a promising drug delivery agent. In this report, its physicochemical properties were assessed in aqueous solution using 1D and 2D ^{1}H NMR spectroscopy. The results showed that the apolar hydrocarbon domain of the gemini surfactant was self-included within the βCD internal cavity. The host/guest complexes composed of native βCD or βCDg with NC 2067 were examined using 1D/2D ROESY NMR methods. The stoichiometry of βCD/NC 2067 complex was estimated using Job's method via ^{1}H NMR spectroscopy. The binding geometry of NC 2067 within βCD was proposed using molecular docking and further supported by 1D and 2D ROESY NMR results. Addition of NC 2067 to βCDg revealed minimal changes to the overall structure of the βCDg system, in agreement with the formation of a βCDg/NC 2067 ternary complex.

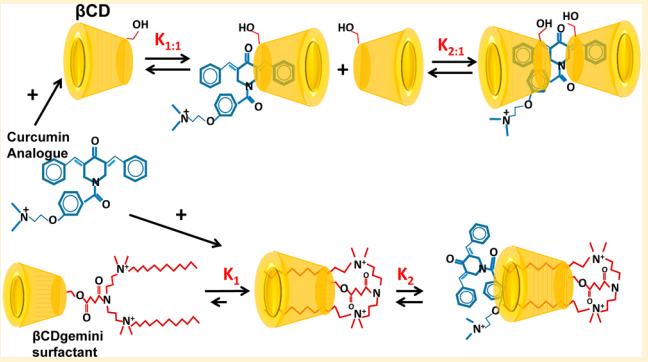

KEYWORDS: *rotating frame Overhauser effect spectroscopy (ROESY), self-inclusion, molecular docking, through-space interaction*

1. INTRODUCTION

β-Cyclodextrin (βCD; Figure 1a) is a toroidal-shaped macrocyclic oligosaccharide composed of seven α-D-glucopyranoside units linked by 1→4 linkages. The macrocycle possesses a hydrophilic outer surface and a lipophilic internal cavity due to its unique molecular structure. βCD and its derivatives have been used widely in pharmaceutical formulations as solubilizing and stabilizing agents. The noncovalent interactions between the βCD host and a hydrophobic drug molecule can result in the formation of stable host/guest inclusion complexes.[1−4] Moreover, CD-based nanoparticles were recently designed by grafting CDs onto polymers,[5,6] by incorporating CDs into liposomes,[7] and through synthesis of amphiphilic βCDs.[8]

Curcumin is an active ingredient of turmeric rhizome and has variable pharmacological activity such as anticancer and anti-inflammatory properties; however, curcumin suffers from poor solubility, instability, and low bioavailability. βCD and its derivatives have been utilized in various studies as carriers for curcumin delivery.[9−13] Recently Jahed et al. evaluated the structure of βCD/curcumin inclusion complex by NMR spectroscopy and molecular modeling.[11] They reported that the aromatic rings of curcumin interact with the internal cavity protons of βCD through hydrophobic forces. In another study, the inclusion complex of a curcumin analogue in βCD at a 2:1 host/guest mole ratio showed an increased *in vivo* anticancer activity.[14] Molecular docking of this complex revealed that the most stable configuration occurred when the curcumin analogue was included through its aromatic rings containing the difluoro and methoxy/hydroxyl groups, where several hydrogen bonds were formed with βCD.[14]

In this study, we selected a curcumin analogue NC 2067 (Figure 1b), as a model guest compound with low water solubility (log P = 4.6) that was previously reported to have high cell toxicity toward the A375 melanoma cell line.[15] A novel modified βCD-based carrier named βCDg (cf. Figure 1c) was

Received: April 2, 2015
Revised: May 31, 2015
Accepted: June 17, 2015
Published: June 17, 2015

DOI: 10.1021/acs.molpharmaceut.5b00261
Mol. Pharmaceutics 2015, 12, 2993−3006

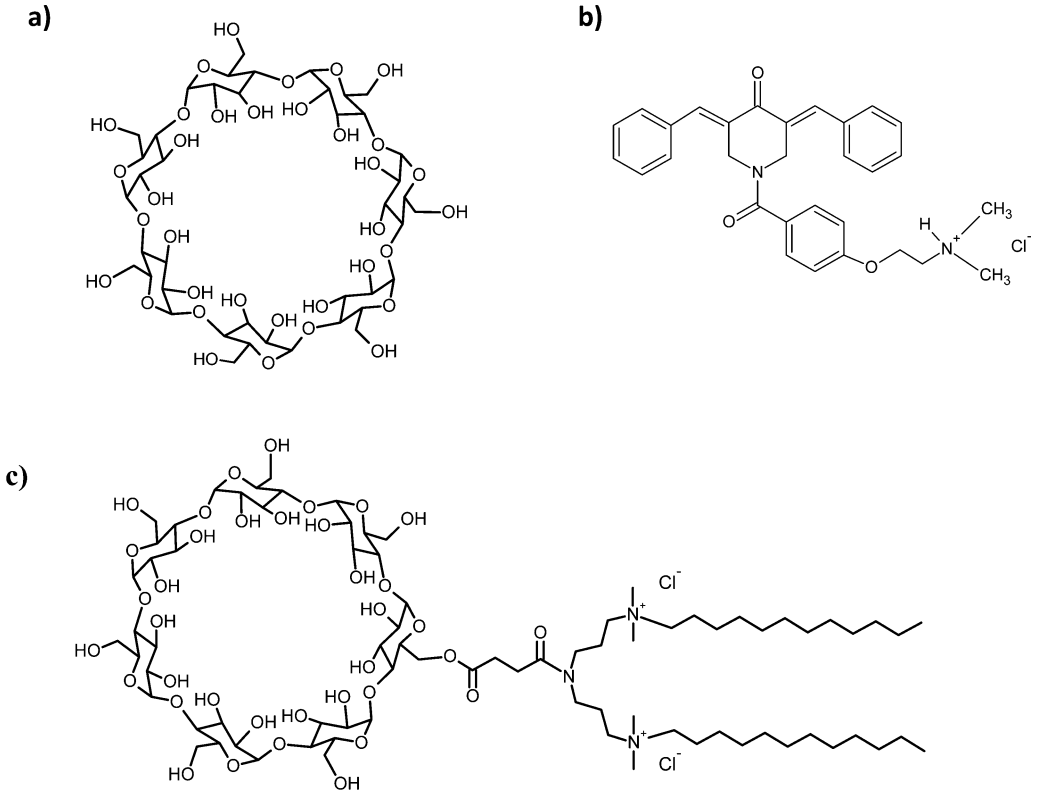

Figure 1. Molecular structures of (a) βCD, (b) NC 2067, and (c) βCDg.

designed to enhance the solubility and bioavailability of NC 2067.[15] This bifunctional surfactant was formed by covalently linking βCD to a gemini surfactant (12-7NH-12) through a succinyl group at the primary hydroxyl group of βCD. In a previous study,[16] the physicochemical characterization of the inclusion complexes of NC 2067 with βCD and βCDg, respectively, was carried out in the solid state using powder X-ray diffraction (PXRD), thermogravimetric analysis (TGA), and Fourier transform infrared spectroscopy (FTIR).

Herein, we report an NMR study in aqueous solution to examine the geometry of the CD-based host/guest systems. The molecular level interactions in solution were elucidated using complexation-induced shift (CIS) data of the ^{1}H nuclei located within the βCD cavity, in the presence and absence of NC 2067. In particular, nuclear Overhauser enhancement (NOE) spectroscopy in the rotating frame (i.e., ROESY) proved to be useful in probing through-space interactions between the host and guest, especially when the proximity of the nuclei is within 4−5 Å.[17] ROESY is exclusively employed for NOE enhancements in molecules with intermediate (∼1000−2000 Da) molecular weight range for host/guest complexes of βCD and small molecules or in molecule systems where the tumbling rates (correlation time) make the measurable NOEs zero or close to zero using conventional NMR methods.[18] ROESY has previously been used to probe the spatial molecular arrangement of the guest in the bound state with CD hosts.[11,19−22] For example, three modes of inclusion of econazole nitrate with βCD derivatives were demonstrated based on the correlation of the βCD interior ^{1}H nuclei with 4-chlorophenyl, 2,4-dichlorophenyl, and imidazole rings, respectively, using NMR results derived from ROESY experiments.[21]

The structure of βCD and βCDg, respectively, with NC 2067 in the bound state was investigated using ^{1}H NMR and 1D selective/2D ROESY NMR spectroscopy. Furthermore, NMR ROESY results were used to monitor changes in the conformation of the self-included gemini surfactant moiety within the βCD cavity upon addition of NC 2067. 1D/2D NMR results were used to provide evidence for the formation of a ternary complex between βCDg and the NC 2067 drug system. The latter provides insight concerning the observed stability of such systems and toward the improved design of delivery agents that are suitable for the formulation of hydrophobic cytotoxic agents.

2. EXPERIMENTAL SECTION

2.1. Materials. βCDg and NC 2067 were synthesized as described elsewhere.[15,23] βCD was purchased from Alfa Aesar (Haverhill, MA, USA). All other chemicals were purchased from Sigma-Aldrich (Oakville, ON, Canada). Complexes of NC 2067 with βCD or βCDg were prepared as described previously.[16] Samples of βCD or βCDg (host) with NC 2067 (guest) were prepared in 2:1 (host/guest) mole ratios by employing variable concentration ratios (2.5:1.25, 5:2.5, and 10:5 mM). The samples were then reconstituted in D_2O, shaken overnight, and analyzed using NMR spectroscopy. The NMR spectrum of gemini surfactant (12-7NH-12) was obtained at 15 mM.

2.2. NMR Spectroscopy. 1D/2D ^{1}H ROESY NMR spectra in solution were recorded on a 500 MHz 3-channel Bruker Avance spectrometer in D_2O at 298 K. Chemical shifts (δ) are reported in ppm with respect to trimethylsilane (TMS; δ 0.0 ppm) as external standard and residual water (HOD; δ 4.79) as an internal standard. Complexation-induced chemical shift (CIS) values were calculated as $\Delta\delta = \delta_{free} - \delta_{complex}$.

DOI: 10.1021/acs.molpharmaceut.5b00261
Mol. Pharmaceutics 2015, 12, 2993−3006

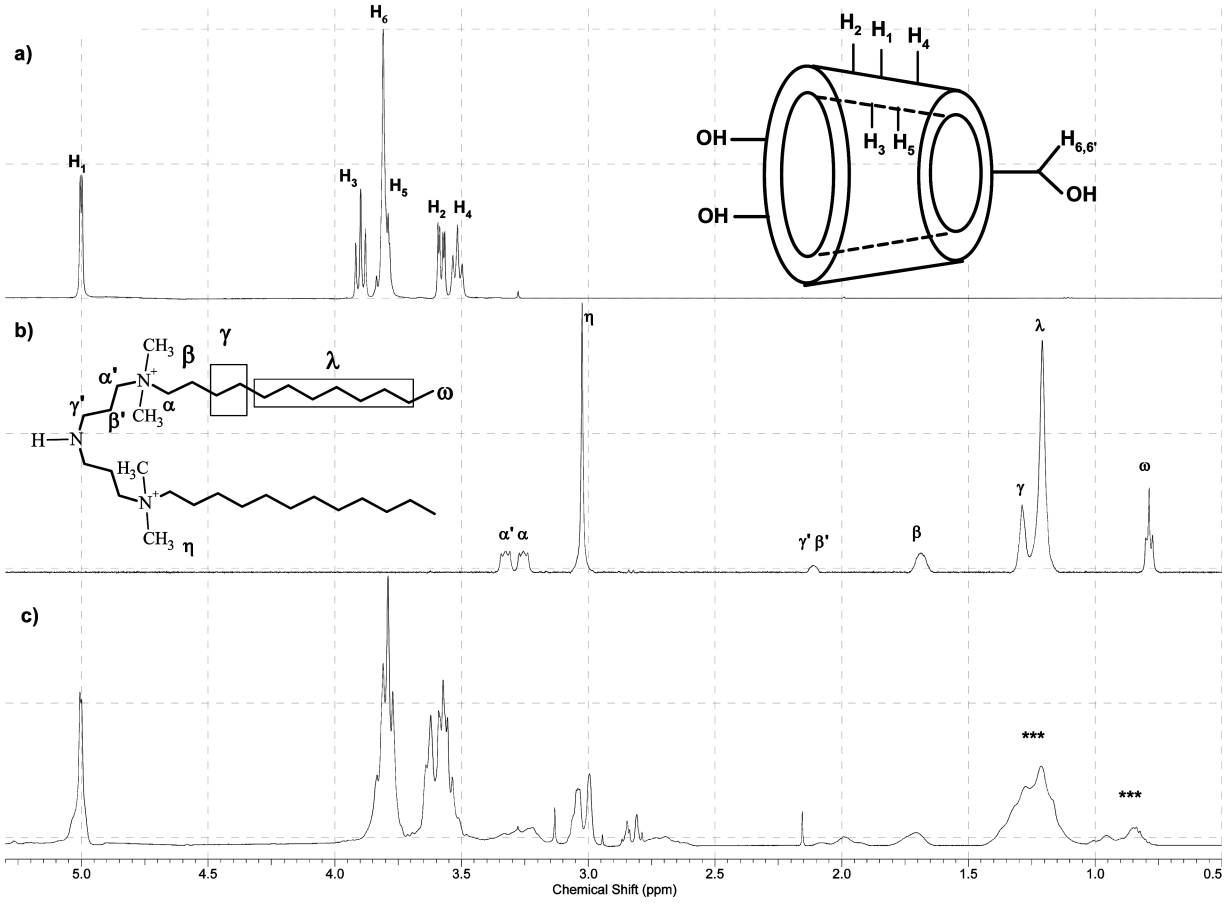

Figure 2. ^{1}H NMR spectra of (a) βCD, (b) gemini surfactant (12-7NH-12), and (c) βCDg obtained in D_2O at 298 K. Broadened resonance lines of the hydrocarbon tail (H_ω, H_λ, and H_γ) of the gemini moiety are shown by asterisks. The relative location of interior and exterior protons of βCD (a) and proton assignment of gemini surfactant (12-7NH-12) (b) are illustrated.

1D selective and 2D ROESY spectra were obtained at variable parameters which were optimized as follows: spin-lock time of 350 ms, recycle delay of 3 s with 8 scans and 1k data points.

2.3. Determination of the Stoichiometry. A series of ten βCD/NC 2067 sample mixtures were prepared in D_2O. The concentration of βCD in the samples was varied from 1 to 10 mM with 1 mM increments, where the sum of the mole concentrations of the βCD/NC 2067 mixtures in each sample was kept constant at 10 mM. The mole fraction r ($0 < r < 1$) was determined based on the ratio of respective mole quantities of βCD to total moles of βCD and drug according to the convention of analysis using Job's plot. Chemical shift changes ($\Delta\delta$) of the internal protons (H_3 and H_5) of βCD were evaluated in each sample, and a graph of $\Delta\delta \times n_{\beta CD}$ versus mole fraction (r) was used to create the Job plot.[24]

2.4. Molecular Modeling. *2.4.1. 3D Structure Optimization.* The molecular structure of βCD was downloaded from the Worldwide Protein Data Bank (PDB: DB03995). The molecular structure of NC 2067 was based on in-house generated single X-ray crystallographic data. Structures were loaded in the Molecular Operating Environment (MOE)[25] software, and hydrogen atoms were subsequently added. The structures were minimized geometrically using the force field function of Merck Molecular Force Field (MMFF94X) and applied in the MOE at a RMS (root-mean-square) gradient of 0.001 Å.

2.4.2. Docking. MOE-based docking consists of five stages: conformational analysis, placement, rescoring (1), refinement, and rescoring (2). In the conformational analysis, a series of torsion angles were applied to the rotatable bonds of the guest (ligand). The alpha triangle was used as a placement method in which the ligand atom triplets and triplets of receptor alpha sphere centers are superimposed. For two stages of scoring, the affinity dG scoring function was used to estimate the impact of enthalpy on the free energy of binding. At the refinement stage the conventional molecular mechanics force field (MMFF94X) was applied for energy minimization. For the first docking run NC 2067 and βCD were set as ligand and receptor, respectively. To estimate the best pose from this run, another βCD was added for the second docking step. Both runs were set to produce 100 poses which were listed and ranked in a database by their relative scoring level in a fashion such that the lowest score was the criterion for the optimized complex. At the end of the cycle, the energy of the docked poses was minimized once again.

3. RESULTS

3.1. ^{1}H NMR and 1D/2D ROESY Characterization of βCDg. To characterize the structure of the bound and unbound host systems, ^{1}H NMR CIS values and NOE effects were used to characterize the βCDg system in solution, as described below.

3.1.1. ^{1}H NMR Spectrum of βCDg. As a prelude to obtaining the ^{1}H NMR spectrum of the βCDg, ^{1}H NMR spectra of βCD

DOI: 10.1021/acs.molpharmaceut.5b00261
Mol. Pharmaceutics 2015, 12, 2993−3006

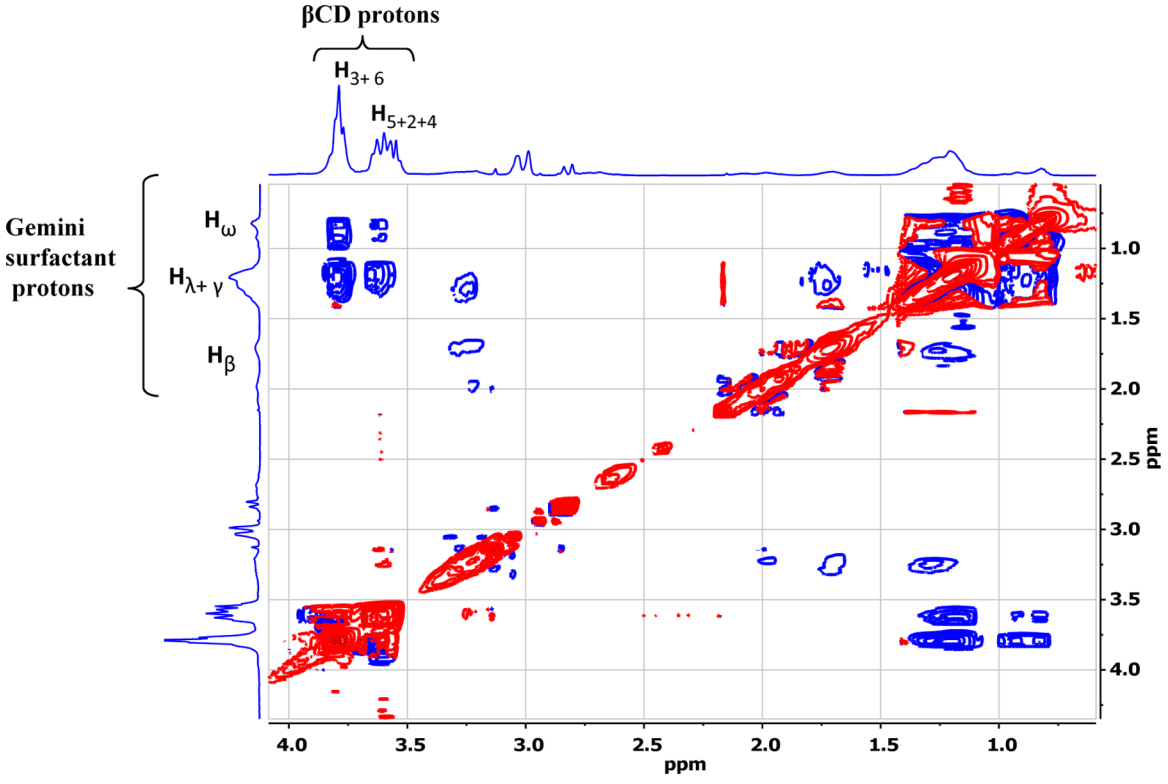

Figure 3. Expansion of the 2D ROESY spectrum of βCDg showing the dipolar cross-peaks between βCD cavity nuclei (H_3, H_5) and the gemini alkyl tail (H_ω, H_λ, and H_γ).

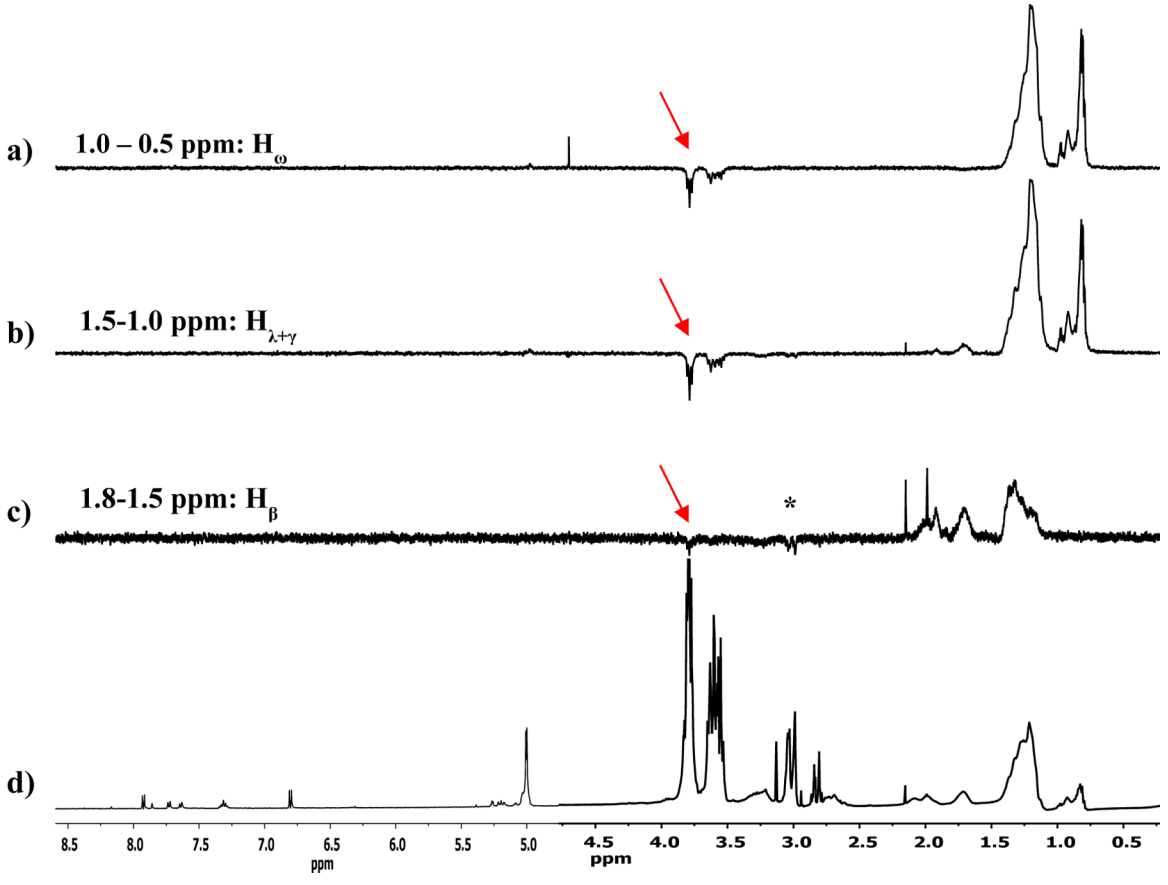

Figure 4. 1D ROESY spectra of βCDg (10 mM) with irradiation of various nuclei: (a) 1.0−0.5 ppm (H_ω), (b) 1.5−1.0 ppm (H_λ and H_γ), (c) 1.8−1.5 ppm (H_β), and (d) 1D ^{1}H NMR spectrum of βCDg. Arrows show inverted peaks due to interaction with the βCD cavity.

DOI: 10.1021/acs.molpharmaceut.5b00261
Mol. Pharmaceutics 2015, 12, 2993−3006

and gemini surfactant (12-7NH-12) were acquired in D_2O for comparison (cf. Figure 2). The structures of βCD and βCD-conjugated gemini surfactant are shown in Figures 1a and 1c, and that of 12-7NH-12 is shown in Figure 2b. The chemical shifts (δ) of the βCD protons (both interior and exterior; cf. Figure 2a) in D_2O are shown in Table S1 in the Supporting Information and are in good agreement with literature values.[26,27] Positive Δδ values indicate upfield shifts and negative Δδ values downfield shifts.

In the ^{1}H NMR spectrum of the βCDg (Figure 2c), the βCD cavity internal protons (H_3 and H_5) showed considerable upfield shift (cf. Table S1 in the Supporting Information). The Δδ values for H_3 (0.094 ppm) and H_5 (0.172 ppm) indicate a partial or complete inclusion of the gemini surfactant moiety within the βCD cavity creating considerable shielding effects. Moreover, the ^{1}H NMR spectrum of the external surface protons (H_4) of the βCD moiety for the βCDg conjugate displayed downfield shifts (Δδ = −0.03 ppm) indicating a deshielding effect for these protons. Furthermore, the H_6 protons at the narrower rim of the βCD cavity showed an upfield shift of 0.019 ppm (cf. Table S1 in the Supporting Information).

The ^{1}H NMR δ values (ppm) of the gemini surfactant (12-7NH-12; cf. Figure 2b) are assigned as listed in Table S2 in the Supporting Information. These results are in good agreement with previous ^{1}H NMR spectral assignments of similar gemini surfactant species.[30] As shown in the spectra of Figure 2, most of the ^{1}H nuclei of the gemini surfactant tail (e.g., H_γ, H_λ, and H_ω) are significantly broadened in the βCDg conjugate relative to the free gemini surfactant (Figure 2, shown by asterisks).

A 1D/2D ROESY NMR study was undertaken to further characterize the structure of the βCD-conjugated gemini surfactant.

3.1.2. 1D/2D ROESY Spectrum of βCDg. A 2D ROESY spectrum for the βCDg system was obtained to further investigate the self-inclusion phenomenon, and the results are shown in Figure 3. Well-defined cross-peaks were observed between the internal protons of βCD (H_3 and H_5) and the protons of the gemini hydrocarbon tails (H_ω, H_λ, and H_γ) (cf. Figure 3).

The greater sensitivity of the 1D ROESY technique offers an option to further confirm the self-inclusion of the gemini alkyl tail within the βCD cavity by selectively irradiating the nuclei of interest. The 1D ROESY results for the βCDg in aqueous solution at 298 K are shown in Figure 4. The inversion of the βCD nuclei between 4.0 and 3.5 ppm was observed due to irradiation of the regions that correspond to H_ω (1.0−0.5 ppm) and $H_{\lambda+\gamma}$ (1.5−1.0 ppm) in Figures 4a and 4b, respectively. Similarly, the excitation of the region corresponding to H_β (1.8−1.5 ppm) showed observable interactions with the βCD cavity nuclei (cf. Figure 4c). This interaction was not evident in the 2D ROESY spectrum and may be attributed to the relatively weak through-space interactions and the conditions under which the ROESY results were obtained for H_ω and $H_{\lambda+\gamma}$. H_β ($2CH_2$) is located closer to the gemini polar headgroup (cf. Figure 2b) and has weaker interactions with the βCD internal cavity as evidenced by through-space interactions with the methyl groups (H_η) on the quaternary ammonium head groups at δ ∼ 3 ppm (cf. Figure 2b, interaction denoted by an asterisk in Figure 4).

3.1.3. Self-Inclusion of the βCDg. The inclusion of the gemini alkyl tail(s) may occur due to self-inclusion (intramolecularly) or by associative interaction between two βCDg (intermolecularly). To understand the nature of the interactions, the chemical shifts of the βCD internal protons (H_3 and H_5) were monitored as a function of concentration of the βCDg. The correlations between concentration and chemical shift changes are shown in Figure 5, where Δδ (ppm) were

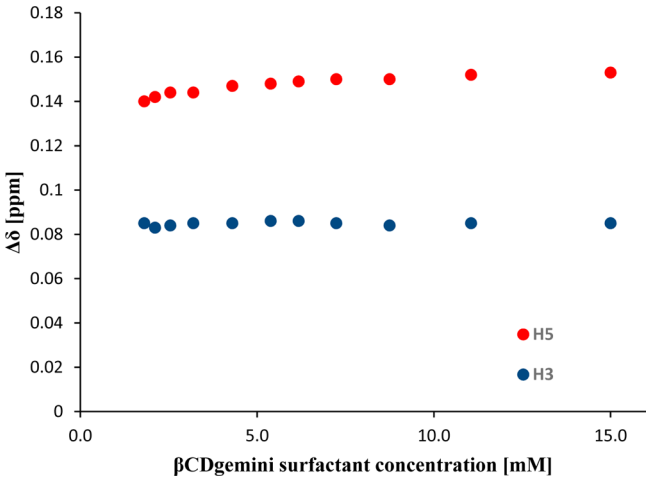

Figure 5. Chemical shift changes of H_3 and H_5 observed at incremental concentrations of βCDg (1 to 15 mM).

computed by subtracting the chemical shift values of unbound βCD from those of βCD-conjugated gemini surfactant. The chemical shift data are presented as Supporting Information (Table S3). The following observations were noted from Figure 5:

(a) No correlations were observed between the chemical shifts changes of H_3 and H_5 and the concentration of βCDg (cf. Figure 5). The foregoing observation suggests that the self-inclusion process of βCDg occurs intramolecularly such that increasing the concentration of βCDg does not lead to proportionately higher chemical shifts of the internal cavity nuclei, as compared with intermolecular association phenomena.

(b) Even though no correlation was observed between the chemical shift changes of H_3 with incremental amount of βCDg, increasing the concentration from 1.8 mM to 15 mM yielded a subtle change of Δδ = 0.013 ppm for H_5 (cf. Figure 5). The weak concentration dependence in Figure 5 could also be interpreted as evidence that intramolecular association (self-inclusion) occurs between the gemini surfactant and βCD cavity.

3.2. ^{1}H NMR and 1D/2D ROESY Characterization of βCD/NC 2067 Complexes. *3.2.1. ^{1}H NMR Spectrum of βCD/NC 2067 Complexes.* The ^{1}H NMR spectra of the complexes of βCD and NC 2067 at a host/guest mole ratio of 2:1 at variable concentrations were obtained and compared to that of free βCD (Figure 6). The ^{1}H NMR spectrum of NC 2067 in D_2O could not be acquired due to its poor solubility in water. The upfield shifts of the cavity protons of βCD (i.e., H_3 and H_5) in Figure 6 indicate a shielding effect due to the inclusion of NC 2067 within the host cavity.

A comparison of the βCD/NC 2067 complex at the highest concentration (10/5 mM) (cf. Figure 6d) showed significant upfield shifts of ∼0.040 and 0.072 ppm for the H_3 and H_5 cavity protons, respectively (cf. Table 1). Increasing the concentration of βCD/NC 2067 from 2.5:1.25 to 10:5 mM resulted in an

DOI: 10.1021/acs.molpharmaceut.5b00261
Mol. Pharmaceutics 2015, 12, 2993−3006

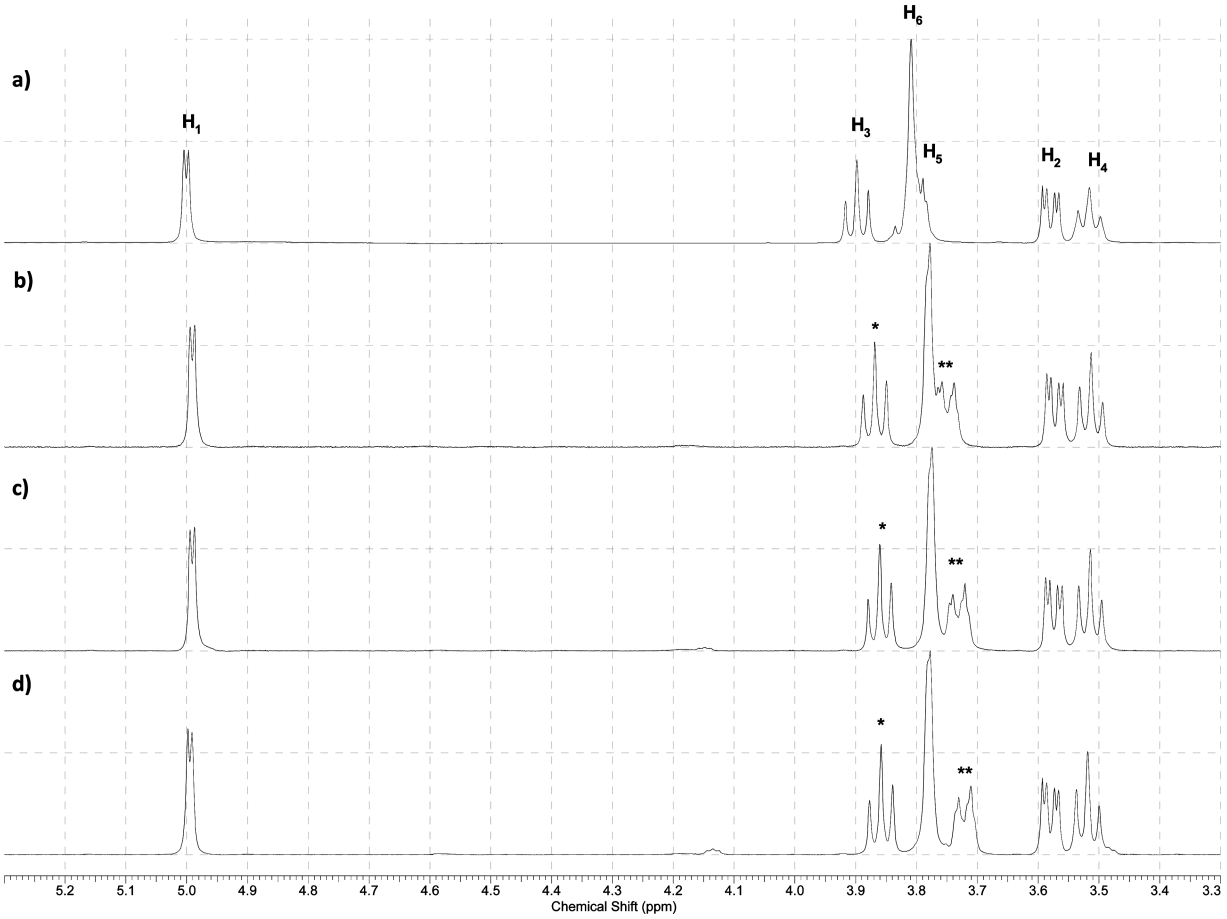

Figure 6. Expansion of ^{1}H NMR spectra of (a) free βCD, and βCD/NC 2067 host/guest complexes at various concentrations of (b) 2.5/1.25 mM, (c) 5/2.5 mM and (d) 10/5 mM collected in D_2O at 298 K. Asterisks correspond to the chemical shifts of H_3 and H_5 for various concentrations of βCD/NC 2067.

Table 1. Chemical Shifts (ppm) for the ^{1}H Nuclei of Unbound βCD and in the Bound State with NC 2067 at Various Concentrations

	δ (ppm): βCD	$\Delta\delta^a$ (ppm): βCD/NC 2067		
	15 mM	2.5/1.25 mM	5/2.5 mM	10/5 mM
H_1	5.001	0.010	0.009	0.006
H_2	3.580	0.007	0.006	0.000
H_3	3.898	0.030	0.038	0.040
H_4	3.516	0.003	0.002	−0.003
H_5	3.803	0.050	0.068	0.072
H_6	3.809	0.031	0.035	0.031

$^a\Delta\delta = \delta_{\beta CD} - \delta_{\beta CD/NC\ 2067}$.

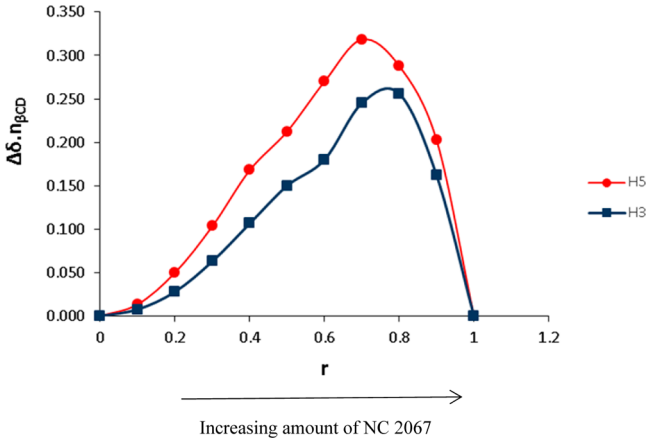

Figure 7. Job's plot of βCD/NC 2067 inclusion complex showing an approximate 2:1 host/guest mole ratio in the complex. Lines on the graph serve as a guide and have no other physical meaning.

increase in the magnitude of $\Delta\delta$ for both H_3 and H_5, suggesting a concentration dependent insertion of NC 2067 in the βCD cavity. Although the inclusion process showed negligible effect on the exterior protons (H_1, H_2, and H_4) of βCD, as expected, the H_6 protons at the narrow face of the cavity also showed an upfield shift of $\Delta\delta \sim 0.02$–0.03 ppm (Table 1).

3.2.2. Stoichiometry of βCD/NC 2067 Complexes. The stoichiometry of the host/guest complex of βCD with NC 2067 was determined using the continuous variation (Job's plot) method.[38] A series of βCD/NC 2067 samples was prepared with different host to guest mole fractions ($0 < r < 1$) where the total concentration was maintained constant. A plot of $\Delta\delta \cdot n_{\beta CD}$ vs mole fraction (r) is shown in Figure 7. The plots showed a maximum value for H_3 and H_5 protons of βCD when $r \sim 0.67$, which corresponds to host/guest mole ratio of 2:1 βCD/NC 2067.[39] 1D/2D ROESY results were studied to further understand the structure of the complexes formed between βCD and the drug (NC 2067).

3.2.3. 1D/2D ROESY Spectra of βCD/NC 2067 Complexes. The 2D ROESY spectrum of βCD/NC 2067 was obtained at 2:1 host/guest ratio (cf. Figure 8). As mentioned above, a

DOI: 10.1021/acs.molpharmaceut.5b00261
Mol. Pharmaceutics 2015, 12, 2993−3006

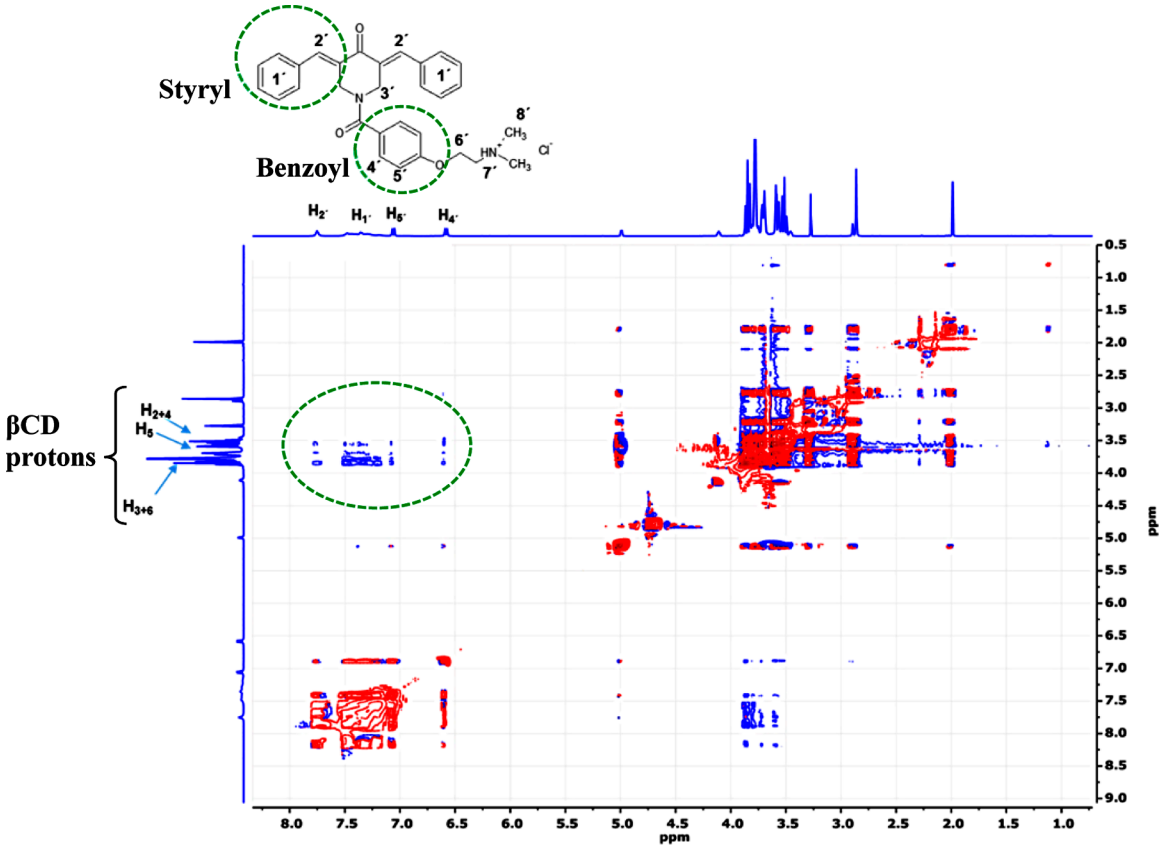

Figure 8. 2D ROESY spectrum of βCD/NC 2067 at a 2:1 host/guest mole ratio (10:5 mM), showing cross-peaks between βCD internal cavity protons and NC 2067 protons.

detailed assignment of the protons of the aromatic rings of free NC 2067 was precluded due to the poor solubility of the drug in D_2O. However, in the presence of βCD the solubility was enhanced such that the ^{1}H NMR signatures were observed in the range of 8.0−6.5 ppm, downfield from the βCD protons (~5.3−3.0 ppm; cf. Figure 8). Moreover, the well resolved 1D spectrum in Figure 8 allowed for the assignment of the NC 2067 peaks to its respective aromatic and alkenic protons. The 2D ROESY spectrum of the βCD/NC 2067 complex showed cross-peaks between H_3 and H_5 protons of the βCD cavity and the styryl protons of NC 2067 ($H_{2'}$ and $H_{1'}$; Figure 8).

The 2D ROESY technique is prone to sensitivity issues when the solubility of the host/guest system is limited or the fraction of bound species is low. Therefore, the host/guest interactions of the βCD/NC 2067 system were further examined using 1D selective ROESY. Various spectral regions of the host or guest were irradiated and the through-space interactions between NC 2067 and βCD were monitored as inverted signals, as shown in Figure 9. Excitation of the region corresponding to the aromatic and alkenic nuclei of NC 2067 (~8.0−6.5 ppm) showed interactions with the βCD cavity (~4.0−3.5 ppm) region (cf. Figure 9a) confirming that the aromatic and alkenic nuclei are bound by the βCD cavity. These results were further confirmed by irradiation of the NC 2067 alkenic guest region (~8.0−7.6 ppm), styryl nuclei (~7.6−7.2 ppm), and the benzoyl moiety (~7.2−6.5 ppm), as shown in Figures 9b, 9c, and 9d, respectively (denoted by arrows).

3.2.4. Molecular Modeling and Mode of Binding of βCD/NC 2067 Complexes. Molecular docking results were performed by MOE to illustrate feasible structures of the complexes for the βCD−drug system. The results were used to complement the experimental findings from the 1D/2D ROESY findings and to establish a better understanding of the complex. The initial docking (NC 2067 and βCD set as ligand and receptor, respectively) of the 1:1 host/guest mole ratio showed the most stable binding mode in which the NC 2067 molecule is included within the cavity of βCD with one of the styryl groups (cf. Figure 10a). This styryl ring is distally remote from the side chain containing the quaternary ammonium group.

The second docking was achieved using the best pose of the first docking attempt in conjunction with a second molecule of βCD, which resulted in a series of poses. The lowest energy (best) pose indicated that the second βCD may encapsulate the unbound styryl ring and the benzoyl ring of the drug at the 2:1 host/guest mole ratio (cf. Figure 10b). The modeling results are in good agreement with the 1D/2D ROESY data (cf. section 3.2.3) and the size−fit requirements of the βCD cavity (262 Å^3) and guest. The interaction of the benzoyl ring ($H_{4'}$ and $H_{5'}$; 7.2−6.5 ppm) occurs with the cavity protons of the second βCD, according to NMR results in Figures 8 and 9.

In Figure 10b, the terminal quaternary ammonium of the side chain of NC 2067 is located outside of the βCD cavity to enable hydration in the solvent phase. However, the carbonyl groups of NC 2067 are positioned between the two βCD rings and form hydrogen bonds with the C_6−OH of βCD. Hydrogen bonds between C_3−OH and C_2−OH at the wider rim and C_6−OH at the narrow rim were observable. It is important to note that the orientation of βCD in the βCD/NC 2067 complex is

DOI: 10.1021/acs.molpharmaceut.5b00261
Mol. Pharmaceutics 2015, 12, 2993−3006

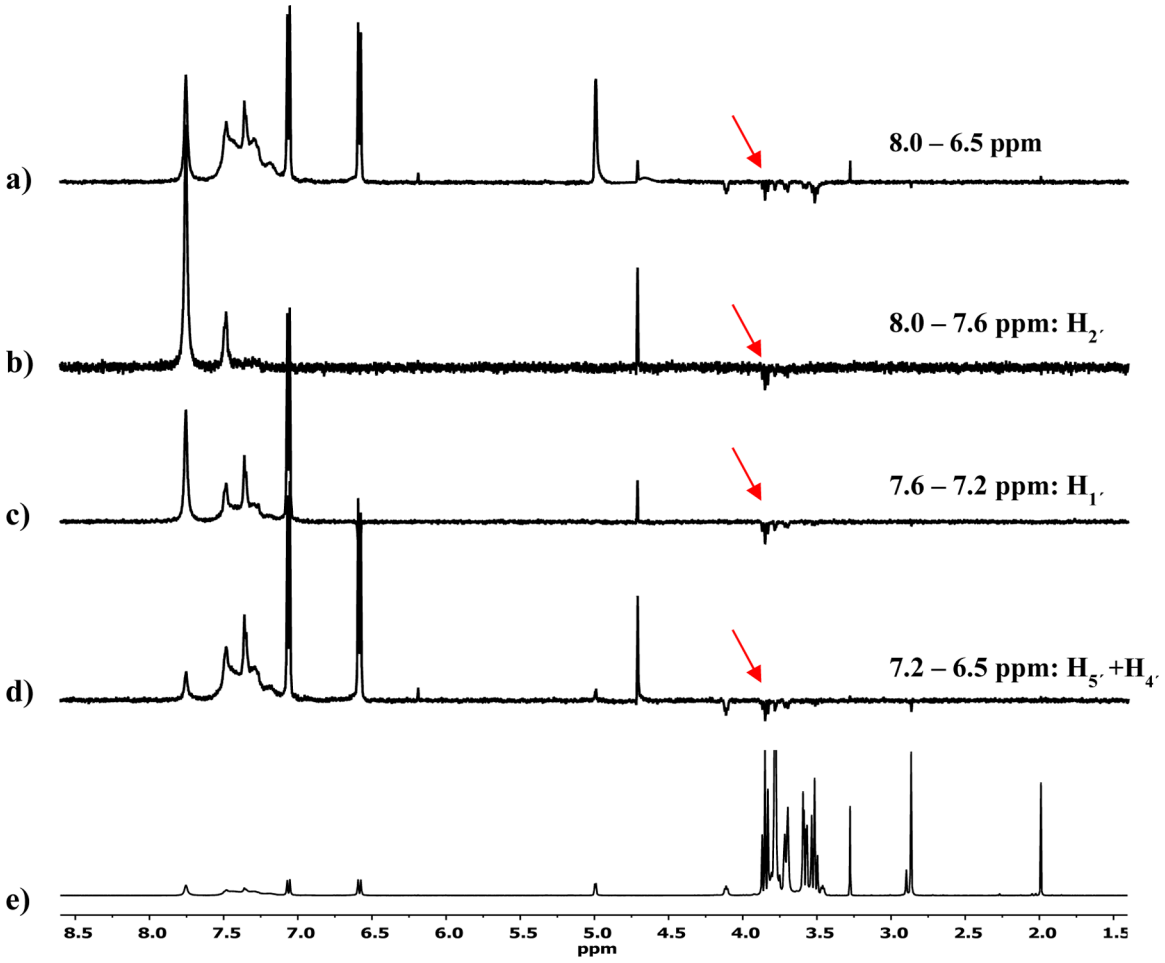

Figure 9. 1D ROESY spectrum of βCD/NC 2067 at a 2:1 host/guest mole ratio (10:5 mM) with irradiation at resonance regions between (a) 8.0 and 6.5 ppm ($H_{2'}$, $H_{1'}$, $H_{5'}$, and $H_{4'}$), (b) 8.0 and 7.6 ppm ($H_{2'}$), (c) 7.6 and 7.2 ppm ($H_{1'}$), and (d) 7.2 and 6.5 ppm ($H_{5'}$ and $H_{4'}$); (e) 1D ^{1}H NMR spectrum of βCD/NC 2067. Arrows show the inverted peaks due to interactions with the βCD cavity.

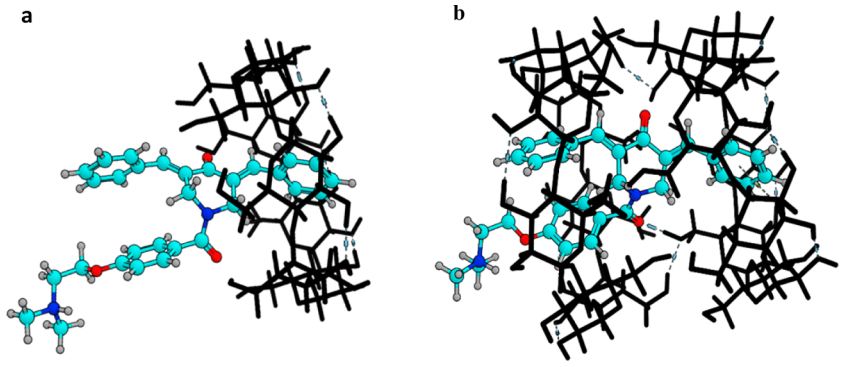

Figure 10. Most stable conformation of βCD/NC 2067 complex at (a) 1:1 and (b) 2:1 host/guest mole ratios. The βCD host is presented as the wire frame model, and the NC 2067 guest is presented as the ball and stick model.

tail to tail, which may also be stabilized by host−host and water mediated H-bonding interactions.

3.3. ^{1}H NMR and 1D/2D ROESY Characterization of NC 2067/βCDg Complexes. *3.3.1. ^{1}H NMR Spectrum of NC 2067/βCDg Complexes.* In order to elucidate the molecular interactions between the βCDg with NC 2067, the ^{1}H NMR spectra of different concentrations of βCDg/NC 2067 at the 2:1 host/guest mole ratio were measured and compared with those of the free βCD and βCDgemini surfactant. The chemical shift data are shown in Table 2, and the ^{1}H NMR spectra are provided as Supporting Information (Figure S1). A detailed assignment of the ^{1}H nuclei of the gemini surfactant moiety of the βCDg was difficult to fully resolve due to the spectral broadening and overlap of the nuclei. The addition of NC 2067 to βCDg did not significantly alter the chemical shifts of the βCDg nuclei at various host/guest concentrations. This is in contrast to the βCDg (section 3.1) and βCD/NC 2067 (section 3.2) systems, which display significant CIS values for H_3 and H_5 nuclei. 1D/2D ROESY measurements were carried out to study the possibility of competing interactions between

DOI: 10.1021/acs.molpharmaceut.5b00261
Mol. Pharmaceutics 2015, 12, 2993−3006

Table 2. Chemical Shifts (ppm) for the ^{1}H Nuclei of βCD in βCDg, Alone without Drug and Various Concentrations of βCDg/NC 2067

		$\Delta\delta^a$ (ppm): βCDg/NC 2067		
	δ (ppm): βCDg	2.5/1.25 mM	5/2.5 mM	10/5 mM
H_1	5.003	0.003	0.001	−0.002
H_2	3.582	−0.010	−0.011	−0.007
H_3	3.804	0.014	0.020	0.002
H_4	3.546	0.004	−0.001	0.003
H_5	3.631	−0.019	−0.009	−0.004
H_6	3.790	0.010	−0.004	−0.003

$^a\Delta\delta = \delta_{\beta CDg} - \delta_{\beta CDg/NC\ 2067}$.

the gemini surfactant alkyl chain and NC 2067 within the βCD cavity of the βCDg/NC 2067complex.

3.3.2. 1D/2D ROESY Results of βCDg/NC 2067 Complexes. The 2D ROESY spectrum of βCDg/NC 2067 (Figure 11) shows cross-peaks between ^{1}H nuclei of the alkyl chain of the βCDg (H_λ, H_γ, and H_ω) and the βCD cavity, similar to the free βCDg in the absence of the drug. However, in contrast to the 2D ROESY results of βCD/NC 2067 system, no interactions of the aromatic protons of the guest drug (8.0−6.5 ppm) with βCD host protons were observed. The most notable feature of the 2D ROESY results of the βCDg/NC 2067 system in Figure 11 are compared with the results of the single component βCDg in Figure 3. The absent (or very weak) interaction of H_ω (gemini tail) with H_5 (βCD cavity) is evidenced by the absence of relevant cross-peaks.

Once again, due to the higher sensitivity of the 1D- versus 2D-ROESY technique, an evaluation of the molecular interactions was estimated from the 1D ROESY spectra for the βCDg/NC 2067 system (Figure 12). Irradiation of the aromatic region (8.0−6.5 ppm) did not result in any spectral inversion (Figure 12a). Similarly, irradiation of the individual areas corresponding to styryl protons of NC 2067 at 8.0−7.6 ppm ($H_{2'}$) and 7.6−7.2 ppm ($H_{1'}$) did not significantly perturb the resonance lines in the 1D spectrum (Figure 12b,c). However, irradiation of the benzoyl group at 7.2−6.5 ppm ($H_{4'}$ and $H_{5'}$) resulted in the inversion of the spectral region corresponding to H_5, H_2, and H_4 (Figure 12d). Irradiation of the gemini tail nuclei (H_ω, $H_{\lambda+\gamma}$, and H_β) between 1.0 and 0.5 ppm, 1.5 and 1.0 ppm, and 1.8 and 1.5 ppm, respectively, resulted in an inversion of the βCD nuclei (cf. Figures 12e, 12f, and 12g). These results are consistent with those for the βCDg in the absence of drug (Figure 4).

4. DISCUSSION

4.1. ^{1}H NMR and 1D/2D ROESY Characterization of βCDg. The significant upfield shifts of the internal protons of the βCD cavity in the ^{1}H NMR spectrum of the βCDg are in agreement with results for well-defined inclusion complexes formed between βCD and alkyl carboxylate anions.[28] Moreover, the downfield shifts of the external protons of the βCD

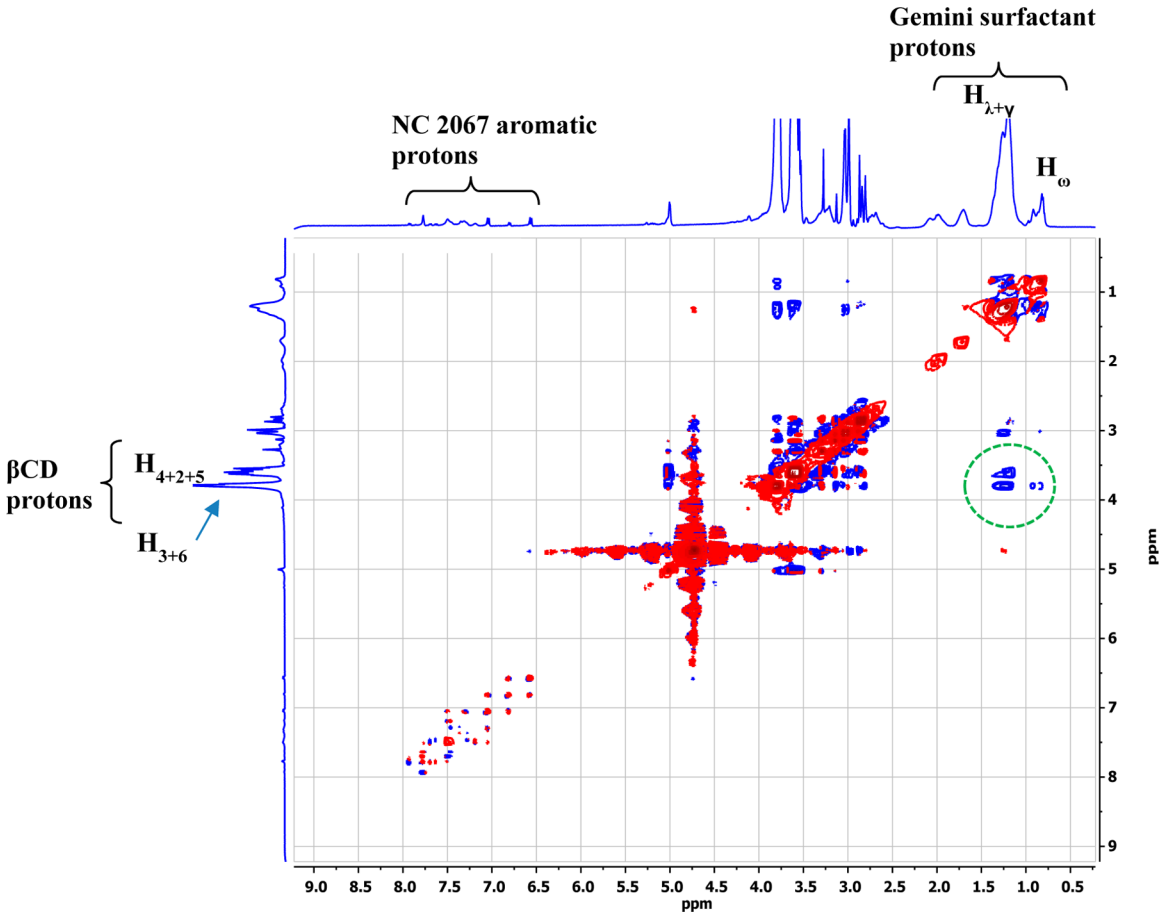

Figure 11. 2D ROESY spectrum of βCDg/NC 2067 at the 2:1 host/guest mole ratio (20:10 mM), showing cross-peaks between the βCD cavity nuclei and the gemini surfactant alkyl tail.

DOI: 10.1021/acs.molpharmaceut.5b00261
Mol. Pharmaceutics 2015, 12, 2993−3006

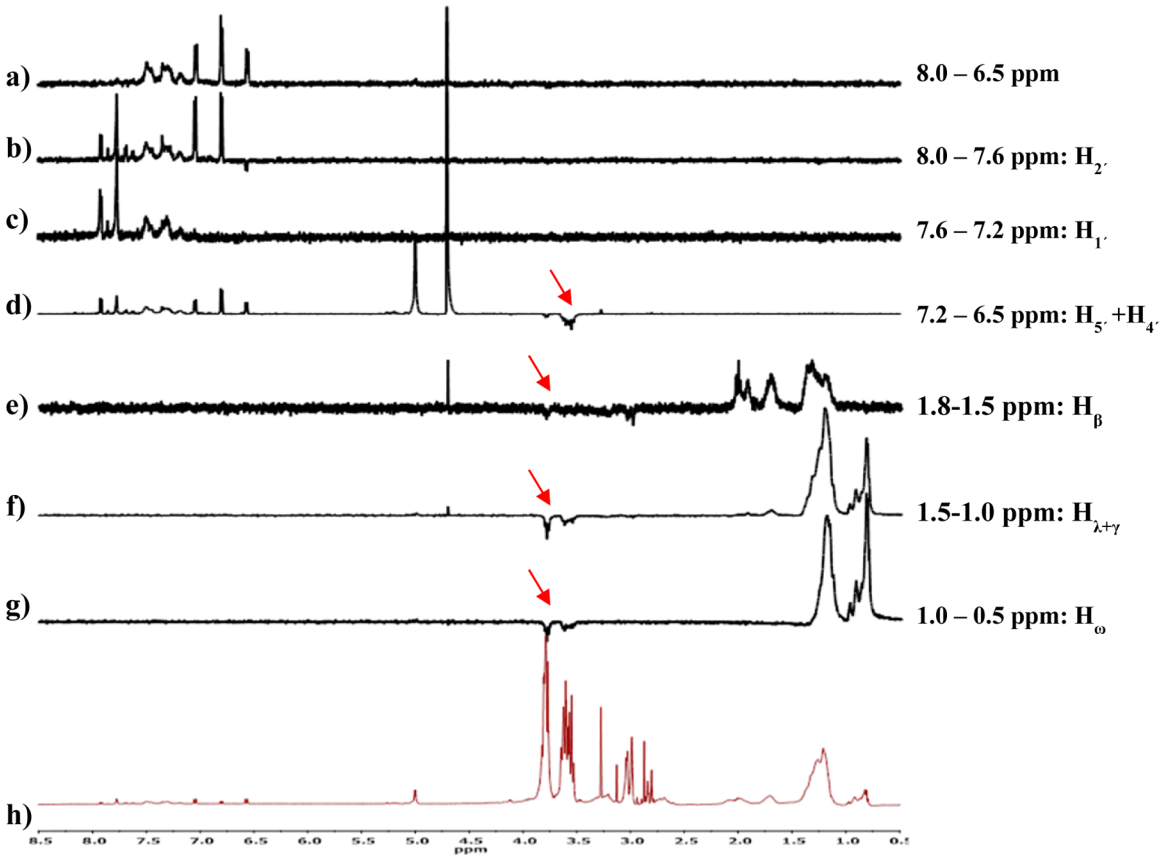

Figure 12. 1D ^{1}H ROESY spectra of βCDg/NC 2067 with irradiation of variable spectral regions between (a) 8.0 and 6.5 ppm (aromatic protons), (b) 8.0 and 7.6 ppm ($H_{2'}$), (c) 7.6 and 7.2 ppm ($H_{1'}$), (d) 7.2 and 6.5 ppm ($H_{5'}$ and $H_{4'}$), (e) 1.8 and 1.5 ppm (H_β), (f) 1.5 and 1.0 ppm (H_λ and H_γ), and (g) 1.0 and 0.5 ppm (H_ω); (h) 1D ^{1}H NMR spectrum of βCDg/NC 2067 (no irradiation). Arrows show the inverted peaks due to dipolar through-space interactions within the complex.

might be related to the proximity of a quaternary ammonium headgroup near the exterior surface of βCD or a combination of conformational effects of the macrocycle. A similar phenomenon was observed in complexes of βCD with gemini surfactants such as 12-OE$_1$-12[29] and 12-s-12.[30] Furthermore, the upfield shift of H_6 protons suggests that the inclusion of the gemini surfactant occurs through the narrower rim of the CD host and is consistent with the grafting of the gemini surfactant moiety at the primary end of the βCD, at the O_6 position, as was confirmed previously.[15]

The broadening of the ^{1}H NMR signatures of the gemini surfactant moiety of the βCDg is consistent with changes in the motional dynamics and hydration states between the bulk solvent and the βCD cavity, and provides further evidence for the interaction of the gemini surfactant with the βCD cavity. The results are similar to a previous study of a monosubstituted βCD with an amphiphilic moiety containing an alkenyl chain, where self-inclusion of the amphiphilic moiety was reported.[31]

Self-inclusion for this system is supported by previous thermogravimetric results of the βCDg system.[16] It was observed that the TGA thermogram of the βCDg did not show any significant water loss at lower temperature (~70 °C) when compared to βCD. The observed differences in hydration suggested that the βCD cavity in βCD-conjugated gemini surfactant was devoid of hydrate water due to self-inclusion of the gemini surfactant moiety. As well, it was found that increasing the concentration of βCDg did not show any overt break point in a plot of specific conductivity vs concentration that is often typical of regular surfactants that undergo self-assembly to form supramolecular structures (e.g., micelles, vesicles, or rods). It was herein hypothesized that the βCD cavity was either fully or partially occupied by the entire or a segment of the alkyl chain of the gemini surfactant moiety, precluding the anticipated self-assembly phenomenon. Moreover, results from small- and wide-angle X-ray scattering did not provide evidence that the gemini surfactant moiety of βCDg underwent formation of self-assembled structures.[16] The latter is in contrast to the formation of self-assembled structures for nonconjugated (conventional) gemini surfactants.[32]

1D and 2D ROESY spectra of the βCDg system indicate that the gemini apolar alkyl chain interacts with the βCD cavity and are consistent with the 1D ^{1}H CIS effects described previously (cf. section 3.1.1). Similarly, it was previously shown that the alkyl tail or spacer of a gemini surfactant is included in the cavity of native βCD according to 2D ROESY results.[29,30]

We found that increasing the concentration of βCDg did not affect the magnitude of the chemical shifts of H_3 and H_5 significantly. This observation indicates that intramolecular interactions occur between βCD and parts of the gemini surfactant. The subtle chemical shift changes observed for H_5 between the highest and lowest concentration of βCDg cannot be used to unequivocally characterize intermolecular interactions.

4.2. ^{1}H NMR and 1D/2D ROESY Characterization of βCD/NC 2067 Complexes. The upfield shifts of the internal protons of βCD in the ^{1}H NMR spectrum of the βCD/NC

DOI: 10.1021/acs.molpharmaceut.5b00261
Mol. Pharmaceutics 2015, 12, 2993−3006

Scheme 1. Illustration of Various Equilibrium Processes for βCD and βCDg Systems[a]

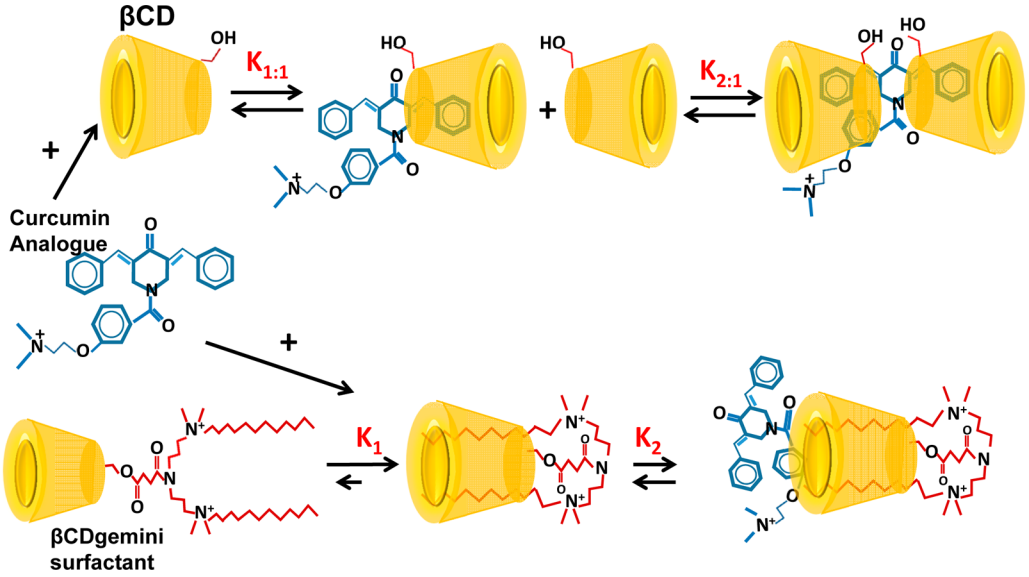

[a]1:1 and 2:1 host/guest complex formation for βCD and NC 2067 (drug), self-inclusion of the alkyl chains of the gemini moiety according to K_1, and the formation of a ternary complex between the self-included form of βCDg and NC 2067 (drug) according to K_2. Solvent is not shown for the sake of clarity. K_2 is assumed to be less than K_1 on the basis of the greater extent of inclusion complex formation for K_1 and the approximate binding affinities of alkyl chains versus phenyl moieties. Further specialized thermodynamic studies are needed to reliably measure the binding constants of the complexes in the future in order to fully characterize the binding properties of these systems.

2067 complex are due to the shielding effects of the apolar phenyl moieties of NC 2067, the anisotropic effect of the π-electrons of the aromatic rings, and displacement of cavity bound water.[33−36] Moreover, the upfield shift of the H_6 protons could be accounted for by changes in rotamer populations of the CH_2 (C_6) due to approach of the NC 2067 aromatic moiety near the annular hydroxyl groups.[37] The results herein indicate that NC 2067 interacts with the βCD cavity without affecting the CIS values of the external cavity protons.

The 2:1 host/guest stoichiometry that was assigned according to the Job's plot is reasonable since there are two styryl ring systems (cf. Figure 1b) which can be bound by two βCD hosts.

The 1D and 2D ROESY spectra of the βCD/NC 2067 complex showed that all aryl protons (ortho, meta, and para) of the styryl group interacted strongly with H_3 protons of the βCD host. The presence of strong cross-peaks for the H_3 protons of βCD was reported elsewhere for the inclusion of fluconazole within βCD through its difluorophenyl moiety.[40] Moreover, it was recently shown from a 2D ROESY study of polymer/dye systems that the phenyl moiety of *p*-nitrophenol was bound by the βCD cavity for a CD-based polymer.[41]

In general, the NC 2067 guest reported herein displays interaction with the cavity protons of βCD at the position of the styryl, alkene, and benzoyl groups (cf. Figure 9). It is not straightforward in this case to unequivocally characterize a well-defined geometry of the bound drug based on the intensity of the cross-peaks for the different nuclei due to broadening effects of the guest signatures. Therefore, the use of molecular modeling may provide an insight regarding the topology of the drug in the bound state with βCD.

Molecular docking results at the first stage showed that a styryl ring interacted with βCD. The noncovalent interactions that occur between the styryl ring of the drug and the βCD cavity (H_3 nuclei) are reasonable based on favorable van der Waals interactions and hydrophobic association. Moreover, the inclusion complexes in which the NC 2067 was inserted in the βCD cavity through the narrower rim were more stable (lower energy) relative to other "poses" where the inclusion was performed from the wider side of the cavity, and this may be understood on the basis of the dipole moment of the βCD macrocycle. It should be noted that hydration contributions may negate such small energy differences.

βCD may encapsulate a second styryl ring and benzoyl ring, while minimizing steric hindrance between each binding site due to the spatial proximity (~4 Å) between the two rings. In addition, the internal diameter of the βCD cavity (6.5 Å) affords inclusion of these two aromatic rings of NC 2067.

Finally, the calculations based on Molecular Operating Environment software provide a basis for rationalizing the size−fit relationship for this host/guest system, however, the global minimum energy for this system may require a fuller account of hydration phenomena. For example, hydrophobic effects are anticipated to be an important driving force in complex formation judging by the relatively low water solubility of the guest (NC 2067).[42]

4.3. ^{1}H NMR and 1D/2D ROESY Characterization of NC 2067/βCDg Complexes. The ^{1}H NMR spectra of βCDg/NC 2067 complexes showed that the variation in the H_3 and H_5 CIS values for the βCDg/NC 2067 system are less apparent. The formation of a ternary complex (βCDg/NC 2067) may result in less pronounced chemical shift changes due to the disordered nature of the complex and the likelihood that the drug is bound in an outer-sphere arrangement. Based on the known binding affinity of βCD/surfactant systems,[28] the binding affinity of the self-included alkyl chain of the βCDg system is likely 10^3 L/mol or greater. By contrast, the binding affinity of the 1:1 complex for the βCD/NC 2067 guest system must be less than or equal to this value since the drug binding by the βCDg does not displace the self-included alkyl tail upon formation of the ternary complex (i.e., βCDg/NC 2067).

DOI: 10.1021/acs.molpharmaceut.5b00261
Mol. Pharmaceutics 2015, 12, 2993−3006

The 1D and 2D ROESY spectra of βCDg/NC 2067 confirmed the interaction of the gemini tail with the βCD cavity. This reinforces the possibility that the gemini alkyl chain has greater affinity for βCD as described above. By contrast, aromatic ring containing compounds ordinarily show binding constants an order of magnitude lower.[11,43] The lack of the cross-peaks of terminal methyl moiety of the gemini tail and βCD cavity provides indirect evidence that the drug may interact with βCDg, further indicating the biological benefit of the complexation.[15,16] The apparent lack of observable interactions between the drug and βCDg host indicates that a noninclusion ternary complex is formed. It is well established that ternary complexes composed of a βCD host and two different guest molecules are known in the case of the coinclusion complexes of pyrene and alcohols with βCD.[44] Therefore, the absence of well-defined cross-peaks between the βCD interior and drug protons is consistent with the possible formation of a ternary complex, as described above. In a previous study by Udachin et al., it was shown that aromatic guests such as pyrene can form noninclusion complexes within the peripheral hydroxyl region of βCD, whereas 1-octanol can be encapsulated within the CD cavity interior according to single crystal X-ray studies.[45] Based on the structure of such ternary complexes, the absence of through-space interactions may be expected due to their disordered nature, in agreement with the broadened lines of NC 2067 in the presence of βCDg (cf. Figure 12).

It appears that the addition of the NC 2067 to βCDg did not reveal any notable spectral changes; however, there is a strong possibility of a weak interaction with the cavity due to formation of a ternary complex as revealed by the interaction of the benzoyl moiety from 1D ROESY results. The gemini surfactant alkyl chain shows stronger affinity for βCD cavity as described above.

The high in vitro activity of the NC 2067 manifested in formulations containing βCDg[15,16] is related to the formation of a weakly bound inclusion complex, in agreement with the idea of an outer-sphere ternary complex for the drug and βCDg. The formation of a ternary complex accounts for the weak interactions, structural disorder of the complex, solubilization phenomena, and bioavailability of NC 2067 with A375 melanoma cells, as depicted in Scheme 1. In addition, the promising results of the in vitro studies such as low toxicity of βCDg[16] and the ability to solubilize the drug and increase the bioavailability with the A375 melanoma cell line illustrate the utility of the βCD-conjugated gemini surfactant to act as a unique drug delivery agent.

4. CONCLUSIONS

In conclusion, three systems were characterized (βCDg, βCD/NC 2067, and βCDg/NC 2067) in order to study the structure of NC 2067 (drug) in βCD-conjugated gemini surfactant complexes. The alkyl tail of the gemini surfactant moiety undergoes intramolecular self-inclusion within the internal cavity of βCD of the βCDg system. The structure of the NC 2067 guest in its complexed form with βCD was evaluated using 1D/2D NMR techniques. The stoichiometry of the βCD/NC 2067 system was estimated to be a 2:1 host/guest complex according to the continuous variation method (Job plot). Moreover, 1D/2D ROESY spectra and molecular modeling indicated that NC 2067 was included by two βCD molecules through its styryl and/or benzoyl groups. By contrast, the addition of NC 2067 to the βCDg resulted in only subtle measurable changes to the system,[16] and that favorable βCDg self-inclusion still persists. The drug (NC 2067) is weakly bound to the βCDg system and likely forms a ternary outer-sphere complex (cf. Scheme 1), in agreement with other related systems,[44,45] including the known stability of loosely bound facial complexes for βCD/guest systems.[46]

The results of this study reveal the behavior of a poorly soluble drug molecule in the presence of complexing/solubilizing agents and represent a major step forward in the design of delivery agents that are safe for the formulation of hydrophobic cytotoxic agents. Future steps will be taken to modify the structure of the βCDg conjugate to control self-inclusion phenomena while promoting drug encapsulation by βCD to afford effective delivery to the target cells. Moreover, grafting of pH-sensitive moieties that facilitate the intracellular release of the drug from the βCDg carrier will also be considered.

■ ASSOCIATED CONTENT

Ⓢ Supporting Information

Additional tables of the chemical shifts for the ^{1}H nuclei of βCD, βCDg, and gemini surfactant (12-7NH-12) and a figure of ^{1}H NMR spectra of βCDg-based systems. The Supporting Information is available free of charge on the ACS Publications website at DOI: 10.1021/acs.molpharmaceut.5b00261.

■ AUTHOR INFORMATION

Corresponding Authors

*I.B.: College of Pharmacy and Nutrition, University of Saskatchewan, Health Sciences Building, 3D01.5, 107 Wiggins Road, Saskatoon, Saskatchewan, S7N 5E5, Canada. Phone: 306-966-6349. Fax: 306-966-6377. E-mail: ildiko.badea@usask.ca.

*L.D.W.: Department of Chemistry, University of Saskatchewan, Thorvaldson 156, Saskatoon, Saskatchewan, S7N 5C9, Canada. Phone: 306-966-2961. E-mail: lee.wilson@usask.ca.

Notes

The authors declare no competing financial interest.

■ ACKNOWLEDGMENTS

M.P. is a fellow of the Canadian Institutes of Health Research Training grant in Health Research Using Synchrotron Techniques (CIHR-THRUST) and thanks the program for financial support. We also thank Dr. Jonathan Dimmock and Dr. Umashankar Das, who synthesized NC 2067. We are grateful for financial support from NSERC and CIHR to carry out this study.

■ REFERENCES

(1) Bender, M. L.; Komiyama, M. *Cyclodextrin chemistry*; Springer-Verlag Berlin: 1978; Vol. *820*.

(2) Connors, K. A. The stability of cyclodextrin complexes in solution. *Chem. Rev.* **1997**, *97* (5), 1325−1357.

(3) Liu, L.; Guo, Q. X. The driving forces in the inclusion complexation of cyclodextrins. *J. Inclusion Phenom.* **2002**, *42* (1−2), 1−14.

(4) Crini, G. Review: A history of cyclodextrins. *Chem. Rev.* **2014**, *114* (21), 10940−10975.

(5) Zhang, J.; Ellsworth, K.; Ma, P. X. Synthesis of β-cyclodextrin containing copolymer via "click" chemistry and its self-assembly in the presence of guest compounds. *Macromol. Rapid Commun.* **2012**, *33* (8), 664−671.

(6) van de Manakker, F.; Vermonden, T.; van Nostrum, C. F.; Hennink, W. E. Cyclodextrin-based polymeric materials: synthesis,

DOI: 10.1021/acs.molpharmaceut.5b00261
Mol. Pharmaceutics 2015, 12, 2993−3006

properties, and pharmaceutical/biomedical applications. *Biomacromolecules* **2009**, *10* (12), 3157−3175.
(7) Agashe, H.; Lagisetty, P.; Sahoo, K.; Bourne, D.; Grady, B.; Awasthi, V. Liposome-encapsulated EF24-HPβCD inclusion complex: A preformulation study and biodistribution in a rat model. *J. Nanopart. Res.* **2011**, *13* (6), 2609−2623.
(8) Sallas, F.; Darcy, R. Amphiphilic cyclodextrins - Advances in synthesis and supramolecular chemistry. *Eur. J. Org. Chem.* **2008**, No. 6, 957−969.
(9) Patro, N. M.; Sultana, A.; Terao, K.; Nakata, D.; Jo, A.; Urano, A.; Ishida, Y.; Gorantla, R. N.; Pandit, V.; Devi, K.; Rohit, S.; Grewal, B. K.; Sophia, E. M.; Suresh, A.; Ekbote, V. K.; Suresh, S. Comparison and correlation of in vitro, in vivo and in silico evaluations of alpha, beta and gamma cyclodextrin complexes of curcumin. *J. Inclusion Phenom. Macrocycl. Chem.* **2014**, *78* (1−4), 471−483.
(10) Mangolim, C. S.; Moriwaki, C.; Nogueira, A. C.; Sato, F.; Baesso, M. L.; Neto, A. M.; Matioli, G. Curcumin-β-cyclodextrin inclusion complex: Stability, solubility, characterisation by FT-IR, FT-Raman, X-ray diffraction and photoacoustic spectroscopy, and food application. *Food Chem.* **2014**, *153*, 361−370.
(11) Jahed, V.; Zarrabi, A.; Bordbar, A. K.; Hafezi, M. S. NMR (1H, ROESY) spectroscopic and molecular modelling investigations of supramolecular complex of β-cyclodextrin and curcumin. *Food Chem.* **2014**, *165*, 241−246.
(12) Ma, M.; Sun, T.; Xing, P.; Li, Z.; Li, S.; Su, J.; Chu, X.; Hao, A. A supramolecular curcumin vesicle and its application in controlling curcumin release. *Colloids Surf., A* **2014**, *459*, 157−165.
(13) Sun, Y.; Du, L.; Liu, Y.; Li, X.; Li, M.; Jin, Y.; Qian, X. Transdermal delivery of the in situ hydrogels of curcumin and its inclusion complexes of hydroxypropyl-β-cyclodextrin for melanoma treatment. *Int. J. Pharm.* **2014**, *469* (1), 31−39.
(14) Dandawate, P. R.; Vyas, A.; Ahmad, A.; Banerjee, S.; Deshpande, J.; Swamy, K. V.; Jamadar, A.; Dumhe-Klaire, A. C.; Padhye, S.; Sarkar, F. H. Inclusion Complex of Novel Curcumin Analogue CDF and β-Cyclodextrin (1:2) and Its Enhanced In Vivo Anticancer Activity Against Pancreatic Cancer. *Pharm. Res.* **2012**, 1−12.
(15) Michel, D.; Chitanda, J. M.; Balogh, R.; Yang, P.; Singh, J.; Das, U.; El-Aneed, A.; Dimmock, J.; Verrall, R.; Badea, I. Design and evaluation of cyclodextrin-based delivery systems to incorporate poorly soluble curcumin analogs for the treatment of melanoma. *Eur. J. Pharm. Biopharm.* **2012**, *81* (3), 548−556.
(16) Poorghorban, M.; Das, U.; Alaidi, O.; Chitanda, J. M.; Michel, D.; Dimmock, J.; Verrall, R.; Grochulski, P.; Badea, I. Characterization of the host−guest complex of a curcumin analog with β-cyclodextrin and β-cyclodextrin−gemini surfactant and evaluation of its anticancer activity. *Int. J. Nanomed.* **2015**, *10*, 503−515.
(17) Neuhaus, D. Nuclear overhauser effect. *Encyclopedia of Magnetic Resonance*; 2000.
(18) Bax, A.; Davis, D. G. Practical aspects of two-dimensional transverse NOE spectroscopy. *J. Magn. Reson. (1969)* **1985**, *63* (1), 207−213.
(19) Yang, L. J.; Ma, S. X.; Zhou, S. Y.; Chen, W.; Yuan, M. W.; Yin, Y. Q.; Yang, X. D. Preparation and characterization of inclusion complexes of naringenin with β-cyclodextrin or its derivative. *Carbohydr. Polym.* **2013**, *98* (1), 861−869.
(20) Yang, L. J.; Yang, B.; Chen, W.; Huang, R.; Yan, S. J.; Lin, J. Host-guest system of nimbin and β-cyclodextrin or its derivatives: Preparation, characterization, inclusion mode, and solubilization. *J. Agric. Food Chem.* **2010**, *58* (15), 8545−8552.
(21) Jug, M.; Mennini, N.; Kövér, K. E.; Mura, P. Comparative analysis of binary and ternary cyclodextrin complexes with econazole nitrate in solution and in solid state. *J. Pharm. Biomed. Anal.* **2014**, *91*, 81−91.
(22) Akita, T.; Matsui, Y.; Yamamoto, T. A 1H NMR titration study on the binding constants for D- and l-tryptophan inclusion complexes with 6-O-α-D-glucosyl-β- cyclodextrin. Formation of 1:1 and 2:1 (host:guest) complexes. *J. Mol. Struct.* **2014**, *1060* (1), 138−141.
(23) Das, U.; Alcorn, J.; Shrivastav, A.; Sharma, R. K.; De Clercq, E.; Balzarini, J.; Dimmock, J. R. Design, synthesis and cytotoxic properties of novel 1-[4-(2-alkylaminoethoxy)phenylcarbonyl]-3,5-bis-(arylidene)-4-piperidones and related compounds. *Eur. J. Med. Chem.* **2007**, *42* (1), 71−80.
(24) Gil, V. M. S.; Oliveira, N. C. On the use of the method of continuous variations. *J. Chem. Educ.* **1990**, *67* (6), 473−478.
(25) Inc., C. C. G. *Molecular Operating Environment*, 2012; Montreal, Quebec, Canada, 2012.
(26) Schneider, H. J.; Hacket, F.; Rüdiger, V.; Ikeda, H. NMR studies of cyclodextrins and cyclodextrin complexes. *Chem. Rev.* **1998**, *98* (5), 1755−1785.
(27) Valente, A. J. M.; Söderman, O. The formation of host-guest complexes between surfactants and cyclodextrins. *Adv. Colloid Interface Sci.* **2014**, *205*, 156−176.
(28) Wilson, L. D.; Verrall, R. E. A 1H NMR study of cyclodextrin - Hydrocarbon surfactant inclusion complexes in aqueous solutions. *Can. J. Chem.* **1998**, *76* (1), 25−34.
(29) Guerrero-Martínez, A.; González-Gaitano, G.; Viñas, M. H.; Tardajos, G. Inclusion complexes between β-cyclodextrin and a gemini surfactant in aqueous solution: An NMR study. *J. Phys. Chem. B* **2006**, *110* (28), 13819−13828.
(30) Carvalho, R. A.; Correia, H. A.; Valente, A. J. M.; Söderman, O.; Nilsson, M. The effect of the head-group spacer length of 12-s-12 gemini surfactants in the host-guest association with β-cyclodextrin. *J. Colloid Interface Sci.* **2011**, *354* (2), 725−732.
(31) Fernando Silva, O.; Fernández, M. A.; Pennies, S. L.; Gil, R. R.; De Rossi, R. H. Synthesis and characterization of an amphiphilic cyclodextrin, a micelle with two recognition sites. *Langmuir* **2008**, *24* (8), 3718−3726.
(32) Foldvari, M.; Badea, I.; Wettig, S.; Verrall, R.; Bagonluri, M. Structural characterization of novel micro- and nano-scale non-viral DNA delivery systems for cutaneous gene therapy. *Technical Proceedings of the 2005 NSTI Nanotechnology Conference and Trade Show*; 2005; Vol. *1*, pp 128−131
(33) Ficarra, R.; Ficarra, P.; Di Bella, M. R.; Raneri, D.; Tommasini, S.; Calabrò, M. L.; Gamberini, M. C.; Rustichelli, C. Study of β-blockers/β-cyclodextrins inclusion complex by NMR, DSC, X-ray and SEM investigation. *J. Pharm. Biomed. Anal.* **2000**, *23* (1), 33−40.
(34) Sinha, V. R.; Anitha, R.; Ghosh, S.; Nanda, A.; Kumria, R. Complexation of celecoxib with β-cyclodextrin: Characterization of the interaction in solution and in solid state. *J. Pharm. Sci.* **2005**, *94* (3), 676−687.
(35) Floare, C. G.; Pirnau, A.; Bogdan, M. 1H NMR spectroscopic characterization of inclusion complexes of tolfenamic and flufenamic acids with β-cyclodextrin. *J. Mol. Struct.* **2013**, *1044*, 72−78.
(36) Upadhyay, S. K.; Ali, S. M. Solution structure of loperamide and β-cyclodextrin inclusion complexes using NMR spectroscopy. *J. Chem. Sci.* **2009**, *121* (4), 521−527.
(37) Wood, D. J.; Hrùska, F. E.; Saenger, W. Proton NMR study of the inclusion of aromatic molecules in. alpha.-cyclodextrin. *J. Am. Chem. Soc.* **1977**, *99* (6), 1735−1740.
(38) Job, P. Spectrographic study of the formation of complexes in solution and their stability. *C. R. Hebd. Seances Acad. Sci.* **1925**, *180*, 928−930.
(39) Hirose, K. A practical guide for the determination of binding constants. *J. Inclusion Phenom.* **2001**, *39* (3−4), 193−209.
(40) Upadhyay, S. K.; Kumar, G. NMR and molecular modelling studies on the interaction of fluconazole with β-cyclodextrin. *Chem. Cent. J.* **2009**, DOI: 10.1186/1752-153X-3-9.
(41) Wilson, L. D.; Guo, R. Preparation and sorption studies of polyester microsphere copolymers containing β-Cyclodextrin. *J. Colloid Interface Sci.* **2012**, *387* (1), 250−261.
(42) Blokzijl, W.; Engberts, J. B. F. N. Hydrophobic effects. Opinions and facts. *Angew. Chem., Int. Ed. Engl.* **1993**, *32* (11), 1545−1579.
(43) Maheshwari, A.; Sharma, M.; Sharma, D. Investigation of the binding of roxatidine acetate hydrochloride with cyclomaltoheptaose (β-cyclodextrin) using IR and NMR spectroscopy. *Carbohydr. Res.* **2011**, *346* (13), 1809−1813.
(44) Muñoz De La Peña, A.; Ndou, T. T.; Zung, J. B.; Greene, K. L.; Live, D. H.; Warner, I. M. Alcohol size as a factor in the ternary

DOI: 10.1021/acs.molpharmaceut.5b00261
Mol. Pharmaceutics 2015, 12, 2993−3006

complexes formed with pyrene and β-cyclodextrin. *J. Am. Chem. Soc.* **1991**, *113* (5), 1572−1577.
(45) Udachin, K. A.; Ripmeester, J. A. A novel mode of inclusion for pyrene in β-cyclodextrin compounds: The crystal structures of β-cyclodextrin with cyclohexanol and pyrene, and with n-octanol and pyrene. *J. Am. Chem. Soc.* **1998**, *120* (5), 1080−1081.
(46) Wilson, L. D.; Verrall, R. E. A Volumetric and NMR Study of Cyclodextrin-Inhalation Anesthetic Complexes in Aqueous Solutions. *Can. J. Chem.* **2015**, *93*, 1−7, dx.doi.org/10.1139/cjc-2014-0549.

DOI: 10.1021/acs.molpharmaceut.5b00261
Mol. Pharmaceutics 2015, 12, 2993−3006